

Simulation of polysilane and polysilyne formation and structure

R.L.C. Vink

Instituut Fysische Informatica, Utrecht University, Leuvenlaan 4, 3508 TD Utrecht, the Netherlands

G.T. Barkema

Theoretical Physics, Utrecht University, Princetonplein 5, 3584 CC Utrecht, the Netherlands

C.A. van Walree and L.W. Jenneskens

Debye Institute, Department of Physical Organic Chemistry, Utrecht University, Padualaan 8, 3584 CH Utrecht, the Netherlands

(October 24, 2018)

We present Monte Carlo simulations of the formation and structure of polysilane, hybrid polysilane/polysilyne and polysilyne networks. The simulation technique allows for the investigation of large networks, containing up to 1000 silicon atoms. Our results show that ring formation is an important factor for all three types of materials. For polysilyne networks, a random structure is found incorporating cyclic substructures, linear chains and branching points.

I. INTRODUCTION

The electronic and optical properties of silicon-based materials are strongly related to the structure of the silicon skeleton and the size and surface properties of the materials [1]. Crystalline silicon, which consists of a three-dimensional silicon framework, is an indirect semi-conductor with a band gap of around 1.10 eV. In other forms of three-dimensional silicon, such as nanocrystalline and porous silicon the band gap is somewhat larger and quasi-indirect, so that rather efficient photo- and electroluminescence have been observed. In contrast, one-dimensional polysilanes ($-\text{SiR}_2-$)_n, which are linear polymers consisting of a backbone of silicon atoms to which two organic side groups R are bonded [2,3] exhibit well-defined, intense absorption and emission bands in the UV spectral region. An interesting aspect of the electronic spectra of polysilanes is that both in the solid state and in solution they are often strongly temperature dependent. This thermochromism finds its origin in conformational changes of the silicon backbone, which is said to be σ -conjugated. Polysilanes are usually synthesized by polymerization of SiR_2Cl_2 monomers, employing alkali metals as coupling agent. The heterogeneous polymerization process is rather complicated, but is proposed to involve both silyl radicals and silyl anions as reactive intermediates [4]. It is noteworthy that in the alkali metal-mediated polymerization there is a tendency to form cyclic oligosilane oligomers.

Organic side chain appended silicon-based materials with a higher dimensionality than polysilanes can be ob-

tained by polymerization of trichlorosilanes RSiCl_3 [5,6]. This yields so-called polysilynes, in which each silicon atom is bonded to three other silicon atoms and to one organic side group R. Polysilynes exhibit a broad indirect semiconductor-like absorption which tails into the visible region [6–8]. The fluorescence, emanating from trapped excitons, is situated in the visible region and has a broad appearance. Hybrid polysilane/polysilyne networks, obtained by polymerization of a mixture of dichloro- and trichlorosilanes, have also been reported [9–12]. These kind of polymers can be viewed as linear polysilanes in which SiR branching points are incorporated. In hybrid polysilane/polysilyne networks the photophysical properties of polysilanes and polysilynes are more or less combined.

Since their discovery, the structure of polysilynes and hybrid polysilane/polysilyne networks has been the subject of debate. Polysilynes were initially assumed to consist of a rigid network of interconnected ring-like structures [6], but it was also argued that they form essentially two-dimensional sheetlike networks [7]. According to another point of view it was reasoned that the growth of a polysilyne preferably occurs at the termini of the polymer chain, which leads to a hyperbranched, dendritic morphology [13]. Cleij *et al.* used PM3 calculations on silyl radicals and silyl anions to show that chain propagation preferentially occurs at the termini of oligo- and polymers and is more likely to occur than branching [14]. It furthermore appeared that formation of silicon ring structures is also an aspect to take into account. Hence, the PM3 calculations led to the idea that polysilynes possess a predominant one-dimensional structure with small branches and incorporated rings.

A number of experimental observations also indicates that polysilynes and hybrid polysilane/polysilynes can be viewed as essentially linear structures. For a series of *n*-hexyl substituted hybrid polysilyne/polysilane networks thermochromism (both in the solid state and in solution), fluorescence and a degree of exciton delocalization were observed which resembled the properties of linear polysilanes [9]. Even more surprising, for a polysilyne with oligo(oxyethylene) side chains in aqueous envi-

ronment thermoresponsive behavior very similar to that of linear polysilanes was found [14]. This thermoresponsive behavior has to originate from folding and unfolding processes of the silicon framework. These results imply that the silicon backbone of polysilynes and hybrid polysilyne/polysilanes are to a certain extent flexible and behave much like one-dimensional systems. Similar conclusions can be drawn from the photophysical properties of well-defined oligosilane dendrimers [15,16].

In this contribution, we present computer simulations of the formation of polysilane, hybrid polysilane-polysilyne networks and polysilynes, and study the properties of the resulting networks. There are three essential characteristics that we included in these simulations: 1) the starting point is a random mixture without any polymerization; 2) monomers diffuse, and when they meet they can form stable bonds; 3) conglomerations of bonded monomers are not stationary and rigid, but they show some diffusion and flexibility. More specifically, in our simulations we implemented the time evolution by means of Monte Carlo dynamics (since the dynamics is overdamped because of the solvent), and the elastic properties of conglomerations were described by an empirical interaction potential featuring bond-stretching and bond-bending, with parameters chosen to match experimental properties of crystalline Si. It is anticipated that a thorough knowledge of the structure of polysilanes and polysilynes gives more insight in the properties of these silicon-based materials.

II. MODEL OF POLYSILANE AND POLYSILYNE

The simulations are started without any trace of polymer present. The only bonds initially present in the system are therefore the internal Si-R bonds shown in Fig. 1. However, in the course of the simulation, as monomers react with each other, Si-Si bonds also form. In these simulations, both the silicon atoms and the alkyl groups are treated as hard spheres with radii r_S and r_R , respectively, see Fig. 1. In the ground state, the Si-R distance is set to r_{RS} and the R-Si-R bond angle to the tetrahedral angle Θ_0 , with $\cos(\Theta_0) = -1/3$. During the simulation, as the monomers diffuse and react, distances and angles are allowed to fluctuate around their ground state values.

In the model, all non-bonded particles interact according to hard-sphere potentials. Bonded particles interact according to the Keating potential [17], which describes the stiffness of the network with respect to bond-length and bond-angle distortions. This potential requires an explicit list of all bonds, and is given by

$$V = \frac{3\alpha}{16} \sum_{\langle ij \rangle} \frac{1}{d_{ij}^2} (\mathbf{r}_{ij} \cdot \mathbf{r}_{ij} - d_{ij}^2)^2$$

$$+ \frac{3\beta}{8} \sum_{\langle jik \rangle} \frac{1}{d_{ij} d_{ik}} \left(\mathbf{r}_{ij} \cdot \mathbf{r}_{ik} + \frac{1}{3} d_{ij} d_{ik} \right)^2, \quad (1)$$

where the summation runs over all pairs and triples in the system; α and β are the bond-stretching and bond-bending force constants, respectively; \mathbf{r}_{ij} is the vector pointing from particle i to particle j and d_{ij} is the ground-state distance between particles i and j ; if these are both silicon atoms, d_{ij} equals r_{SS} , otherwise one particle is a silicon atom and the other an alkyl fragment, and d_{ij} equals the equilibrium Si-R distance r_{RS} in that case. The values for the parameters used in the simulation are listed in Table I.

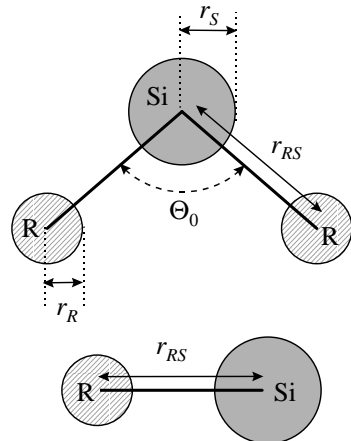


FIG. 1. Diagrammatic representation of SiR_2 (top) and SiR fragments (bottom). Silicon atoms are labeled 'Si', alkyl groups 'R'. Their respective radii are r_S and r_R . The ground state Si-R distance is set r_{RS} and the ground state R-Si-R angle in silane to the tetrahedral angle Θ_0 .

III. SIMULATION DYNAMICS

The simulation starts with a configuration of n_2 SiR_2 and n_3 SiR monomers, placed at random positions and with random orientations in a periodic box, under the constraint of the hard-sphere interactions. The size of the box is chosen such that the particle density equals $2.0 \cdot 10^{-4}$ monomers per \AA^3 , matching the experimental conditions where typically 20 mmol of monomer is put into a reaction volume of 60 ml [9]. The nature of the dynamics is two-fold: monomer diffusion and reactions between monomers. We simulate this with the approach of rare-event dynamics [18]. In this approach, the two types of events are monomer displacements, which occur with a rate r_1 , or bond formation between two silicon atoms, which occur with a rate r_2 . This reaction can only occur when (1) both Si atoms are not saturated, i.e., they have less than four bonds to either alkyl-groups or other silicon atoms, (2) the silicon atoms are separated

less than a cut-off distance r_c , and (3) the silicon atoms are not mutually bonded already. We continue to simulate until reactions become rare. This occurs when approximately 80% of all possible Si-Si bonds have formed. We then investigate the structure of the final network.

When concentrating on the final structure, the overall scaling of the rates r_1 and r_2 is irrelevant, since it only affects the time scale of the simulation. The networks presented here were generated using $r_1 : r_2 = 5 : 1$. To the best of our knowledge, no experimental data on the reaction rates r_1 and r_2 are reported. However, we have established that the networks are insensitive to the ratio of rates. For $r_1 : r_2 = 1 : 2$ and $1 : 10$, we obtained similar results.

We recall that polysilanes are formed by silicon atoms bonded to two alkyl groups, and polysilynes by silicon atoms bonded to one alkyl group. Therefore, a system consisting of n_2 SiR₂ and n_3 SiR monomers is represented by a total number of $N \equiv 3n_2 + 2n_3$ locations in three-dimensional space. We denote the total number of pairs of silicon atoms that are able to react as P , a quantity that varies during the simulation. In terms of N and P , the total diffusion rate R_1 can be written as $R_1 = r_1 N$, the total reaction rate R_2 as $R_2 = r_2 P$, and the total rate of events as $R_1 + R_2$. Events are selected one-at-a-time. To each event, a time-increment of $\Delta t = 1/(R_1 + R_2)$ is attributed. The likelihood that this event is a diffusion event or a reaction event, is equal to $R_1 \Delta t$ and $R_2 \Delta t$, respectively.

To describe the diffusion process, we introduce the following event:

1. We select randomly one silicon atom or alkyl group.
2. For this silicon atom or alkyl group, a displacement is proposed, drawn randomly from within a sphere with radius r_m .
3. If the hard-sphere constraints are violated, the proposed displacement is rejected. Otherwise, the displacement is accepted with the Metropolis acceptance probability [19]

$$P_m = \min \left[1, \exp \left(\frac{E_b - E_f}{k_b T} \right) \right], \quad (2)$$

where k_b is the Boltzmann constant, T is the temperature, and E_b and E_f are the total (Keating) energies of the system before and after the random displacement.

Since we displace single silicon atoms and alkyl groups, the above procedure also allows for the vibration and rotation of monomers.

To describe reactions in the simulation, we introduce the following reaction event:

1. We select randomly one of the P pairs of silicon atoms able to react.

2. A bond is placed between the two silicon atoms constituting the selected pair.

IV. RESULTS

Polysilane networks, polysilyne networks and hybrid polysilane-polysilyne networks are obtained using the simulation method described above. Each system contains a total of 1000 monomers. To characterize the structure of these networks, we proceed as follows. First, we identify clusters, defined as a group of connected monomers. For each cluster, we calculate its genus g given by $g = 1 + e - n$, where e is the number of Si-Si bonds in the cluster and n the number of silicon atoms in the cluster. The genus helps to identify the topology of the cluster: it measures the number of bonds that can be cut before the cluster loses its connectivity. For example, if $g = 0$, the cluster is a chain of connected monomers, i.e. a polymer, and if $g = 1$, the cluster is a ring, possibly with a number of side-chains attached. Networks with high values of g have a complicated topology.

A. Polysilane

We performed one simulation containing 1000 SiR₂ and no SiR fragments at a density of $2.0 \cdot 10^{-4}$ monomers per Å³. The final network is shown in Fig. 2; 86.9% of all possible Si-Si bonds are formed.

TABLE I. Values of parameters used in the simulation: r_{RS} and r_{SS} are the ground state Si-R and Si-Si distances, respectively, and r_s and r_R are the radii of a silicon atom and an alkyl group, respectively; values for these four parameters were adapted from an MM2-calculated structure of dodecamethylcyclohexasilane. Reactions between two silicon atoms can occur only when their separation is less than r_c . r_m is the maximum particle displacement during a diffusion step. α and β are the standard Keating parameters [17]. T is the temperature; r_1 and r_2 are the rates of diffusion and reaction, respectively.

| | | |
|-------------|-------|--------------------|
| r_{RS} | 1.89 | Å |
| r_{SS} | 2.35 | Å |
| r_s | 1.20 | Å |
| r_R | 1.10 | Å |
| r_c | 2.50 | Å |
| r_m | 0.30 | Å |
| α | 2.965 | eV Å ⁻² |
| β | 0.845 | eV Å ⁻² |
| T | 293.0 | K |
| $r_1 : r_2$ | 5 : 1 | |

Since silane is bifunctional, only two types of structure exist in this case: chains (polymers) with $g = 0$ and rings with $g = 1$. The network consists of 228 separate clusters, ranging in size from one up to twelve silicon atoms. Of these clusters, 131 are chains, the remainder are rings. Polymer length and ring size statistics are shown in Fig. 3. In our simulation, 46.8% of the silane monomers form linear structures; a substantial fraction of 53.2% of the monomers is found in rings. For this system, the Si-R and the Si-Si bond lengths are $2.10 \pm 0.07 \text{ \AA}$ and $2.32 \pm 0.08 \text{ \AA}$. The R-Si-R and Si-Si-Si bond angles are 107.0 ± 5.1 and 109.7 ± 7.9 degrees, respectively.

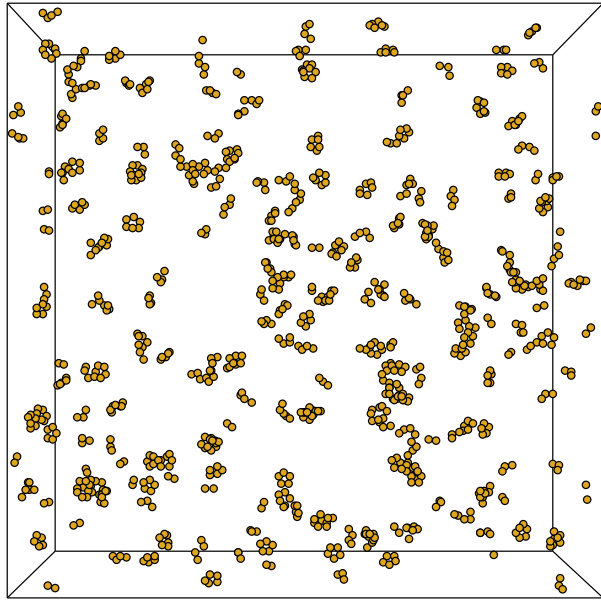


FIG. 2. Resulting polysilane structure at density $2.0 \cdot 10^{-4}$ monomers per \AA^3 . For clarity, the alkyl groups are not shown.

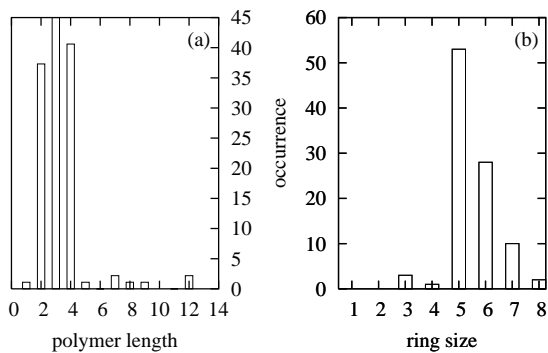


FIG. 3. Histograms showing polymer length (a) and ring size distribution (b) for polysilane consisting of 1000 monomers at density $2.0 \cdot 10^{-4}$ fragments per \AA^3 .

To study the effect of the monomer density, an additional polysilane is simulated at an increased density of $5.0 \cdot 10^{-3}$ monomers per \AA^3 . This network is shown in Fig. 4; 92.3% of all Si-Si bonds are formed. In this case,

the system contains 104 separate clusters, ranging in size from two up to 36 silicon atoms. Of these clusters, 77 are incorporated in linear structures, the remainder form rings. Fig. 5 shows the polymer length and ring size distributions. In this simulation, 84.2% of the silane fragments form linear structures; the remainder form rings. For this system, the Si-R and the Si-Si bond lengths are $2.09 \pm 0.07 \text{ \AA}$ and $2.32 \pm 0.08 \text{ \AA}$. The R-Si-R and Si-Si-Si bond angles are 107.2 ± 5.0 and 111.1 ± 6.7 degrees, respectively.

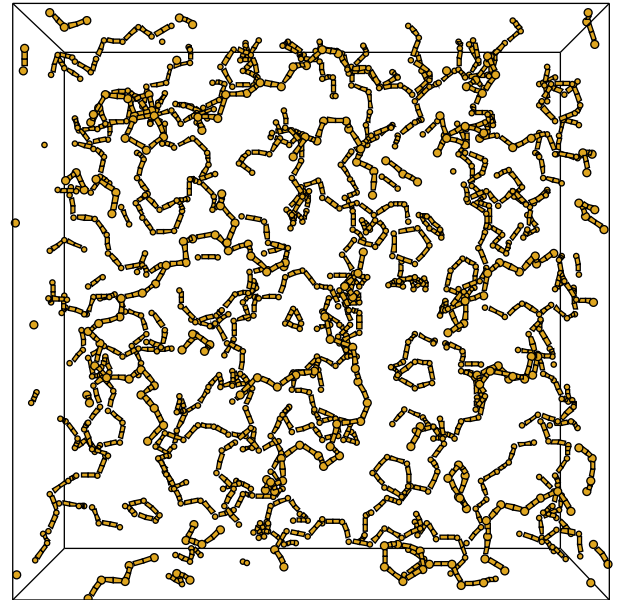


FIG. 4. Resulting polysilane structure at density $5.0 \cdot 10^{-3}$ monomers per \AA^3 . For clarity, the alkyl groups are not shown.

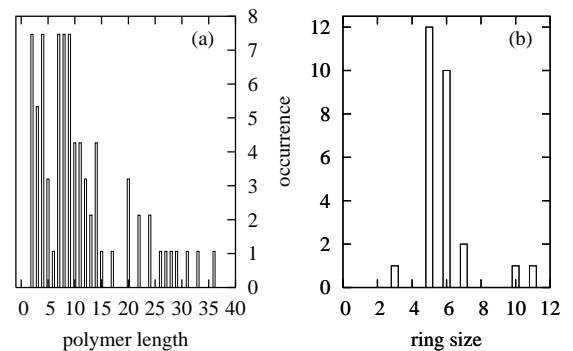


FIG. 5. Histograms showing polymer length (a) and ring size statistics (b) for polysilane consisting of 1000 monomers at density $5.0 \cdot 10^{-3}$ monomers per \AA^3 .

B. Polysilyne

We also performed one simulation involving 1000 SiR monomers, no SiR₂ monomers being present at a density

of $2.0 \cdot 10^{-4}$ monomer fragments per \AA^3 . The final network is shown in Fig. 6; 77.9% of all possible Si-Si bonds were formed. Since silyne is trifunctional, the genus of the structures can now reach large values. The final network consists of 96 separate clusters, ranging in size from two up to 29 monomers. Fig. 7 shows a histogram of the cluster sizes. Of these clusters, only three are chains, 31 possess a monocyclic structure and the remaining are structures with $g > 1$. Fig 7b shows a histogram of the genus numbers. The structure is not dendritic: by far the largest fraction of monomers are part of rings; the fraction of monomers in chains or side-chains is 5.6% only. Moreover, the chains and side-chains are short, consisting at most of three monomers. For this network, the Si-R and the Si-Si bond lengths are $2.09 \pm 0.08 \text{\AA}$ and $2.33 \pm 0.09 \text{\AA}$, respectively. The Si-Si-Si bond angle is 106.7 ± 10.0 degrees.

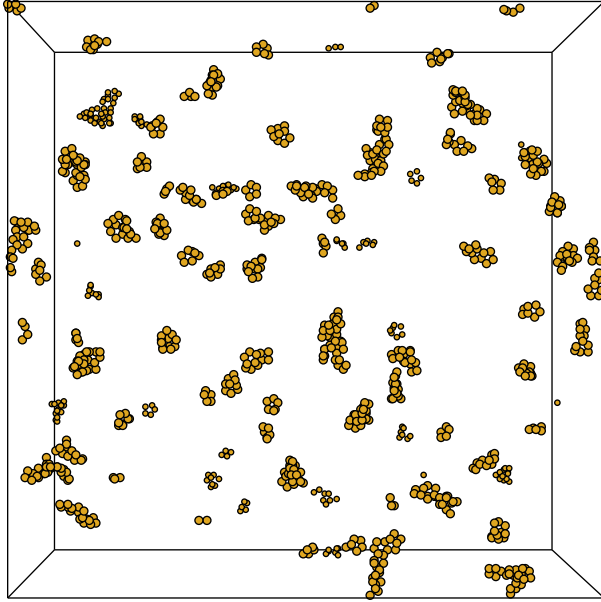


FIG. 6. Polsilyne network at a density of $2.0 \cdot 10^{-4}$ monomers per \AA^3 . For clarity, the alkyl groups are not shown.

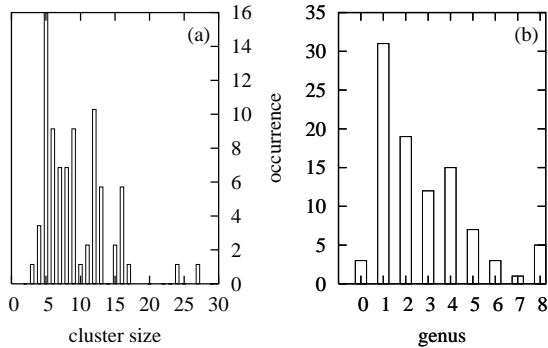


FIG. 7. Histogram of cluster size (a) and genus number (b) of a silyne network consisting of 1000 monomers at density $2.0 \cdot 10^{-4}$ monomers per \AA^3 .

To study the effect of the monomer density, an additional silyne network is generated at an increased density of $8.0 \cdot 10^{-3}$ monomers per \AA^3 . This network is shown in Fig. 8. In this case, 88.8% of all possible Si-Si bonds are formed. All monomers form one large cluster with a genus of 333. The structure consists mostly of connected rings; 94.4% of the monomers are part of rings. The ring statistics are shown in Fig. 9.

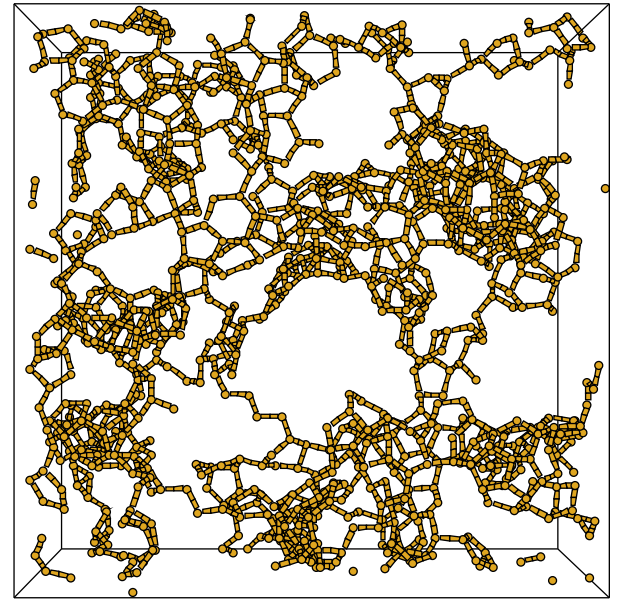


FIG. 8. Polsilyne network at a density of $8.0 \cdot 10^{-3}$ monomers per \AA^3 . For clarity, the alkyl groups are not shown.

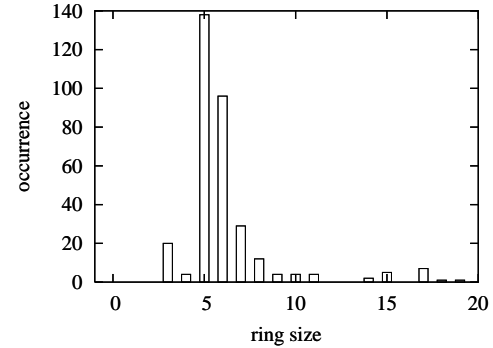


FIG. 9. Ring size histogram for a polsilyne cluster consisting of 1000 monomers. This cluster was generated at a density of $8.0 \cdot 10^{-3}$ monomers per \AA^3 .

C. Hybrid silane/silyne networks

We also performed simulations of hybrid silane/silyne networks, either rich in silylene units (containing 800 SiR_2 and 200 SiR monomers) or rich in branching points (containing 200 SiR_2 and 800 SiR monomers). The density was $2.0 \cdot 10^{-4}$ monomers per \AA^3 . For both net-

works, approximately 80% of the possible Si-Si bonds are formed. The SiR_2 -rich network consists of 175 separate clusters, ranging in size from one up to 17 monomers. In Fig. 10a, a histogram of the cluster sizes is shown. Of these clusters, 60 are linear structures, 98 are rings, the rest are structures with $g > 1$. See Fig. 10b for a histogram of the genus numbers found. For this network, the typical chain length ranges from two to four monomers; rings consist typically of five to six silicon atoms.

The silyne-rich network consists of 108 separate clusters, ranging in size from one up to 37 monomers. In Fig. 11a, we show a histogram of the cluster sizes found. Of these clusters, 17 are linear structures, 31 are rings, the rest are structures with $g > 1$. See Fig. 11b for a histogram of the genus numbers found. For this network, the typical chain length is two monomers; rings typically contain five to six silicon atoms.

Both networks show structures that are not dendritic. For the silane-rich network, 31.8% of the monomers form chains. For the silyne-rich network, this fraction is 11.6%. Most of the monomers are incorporated in rings.

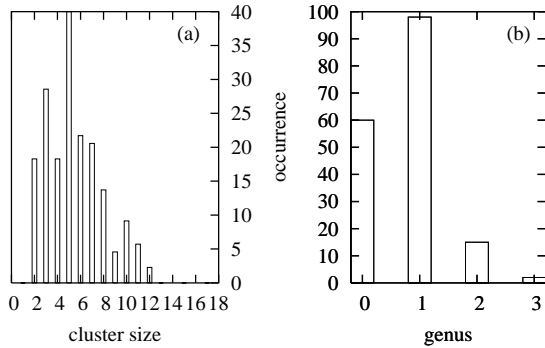


FIG. 10. Histogram of cluster size (a) and genus number (b) for a silane-rich network, consisting of 800 silane and 200 silyne monomers.

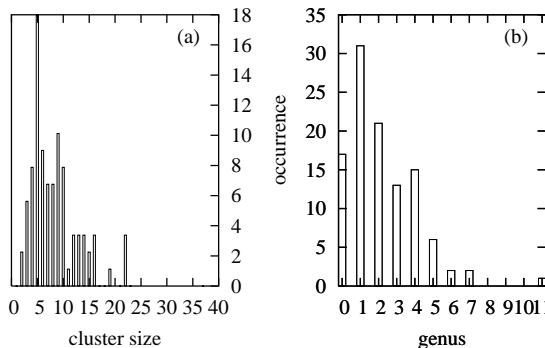


FIG. 11. Histogram of cluster size (a) and genus number (b) for a silyne-rich network, consisting of 200 silane and 800 silyne monomers.

V. DISCUSSION AND CONCLUSION

The Wurtz-type polymerization of dichlorodialkylsilanes and trichloroalkylsilanes is a complex process [2–4]. The polymerization proceeds by a chain growth process at the alkali metal surface, which plays an essential role in the formation of polymers of high molecular weight. This is for instance indicated by the fact that employment of homogeneous coupling agents leads to formation of only oligomeric materials [3,20]. Which products actually are obtained also depends on parameters as the nature of the alkali metal, the solvent and the type of organic side chain. Moreover, after the initial stages of the formation of linear polymers, secondary reactions including depolymerization, backbiting by silyl anions and redistribution of chain lengths are known to occur [2–4]. For polysilynes, secondary reactions such as ring opening reactions (by analogy with spirosilanes, see Ref. [13]), ring-size redistribution and coupling to linear moieties may be of interest. It is a virtually impossible task to perform a simulation of a Wurtz-type polymerization at a metal surface, hereby also taking all these contributing factors into account. Nevertheless, as the approach we used led to results which adequately reflect experimental findings, we believe that our results are sound and provide insight into the structure and properties of polysilanes, polysilynes and hybrid polysilane/polysilane networks.

For polysilane, for instance, the simulations adequately predict the effect of the monomer density on the nature of the silicon compounds formed. At low density, the system has a strong tendency to form five- and six-membered rings, see Fig. 3. This finding is in accordance with the experimental observation that formation of cyclic silicon-based compounds is favored by slow addition of the monomer to the alkali metal, i.e. by maintaining a low monomer concentration [21,22]. The ring size distribution shown in Fig. 3, which indicates that five-membered rings are formed in excess, is in agreement with the experimental distribution such as obtained upon reaction of a dialkyldichlorosilane under kinetic control [2]. It is noteworthy that in an equilibrium distribution, which arises from redistribution of the kinetic mixture upon use of excess alkali metal, the six-membered ring dominates. As expected, the amount of long linear fragments increases strongly when the monomer density is increased, see Fig. 5. At this higher concentration five- and six-membered rings are formed in equal amounts. Furthermore, the length of the linear fragments is rather moderate, which may support the idea that the presence of an alkali metal surface is essential for the formation of high molecular weight polymers [3,20].

For the polysilyne, the simulations also predict the formation of cyclic structures, see Figs. 6–9. At low concentration virtually all monomers are incorporated

into rings. Notwithstanding that monocyclic systems are formed in the largest amount, the number of mutually bonded rings is already considerable. At high monomer density, a very complex network of genus 333 is obtained. Of the monomers, 94.4% is incorporated in rings, which mainly contain five or six silicon atoms. Thus, whereas in the linear case a higher concentration leads to a larger amount of linear structures, for the polysilynes the silicon atoms are still virtually exclusively found in cyclic structures. A few linear fragments are however also present. The simulated structure is in close agreement with the characteristics of the material that was isolated after the first stage of a polymerization of trichloroalkyl-silanes [23]. Our simulations indicate that the structure of polysilynes can be viewed as a network of silicon atoms comprising fused cyclic structures and cyclic structures mutually connected by a single Si-Si bond. There is neither indication of formation of a regular sheetlike arrangement of silicon atoms [7] nor of a dendritic structure [13], at least in our simulations where there is no difference in reactivity between Si-SiCl-Si groups and terminal SiCl groups.

The results obtained for the hybrid polysilane / polysilyne networks do not substantially differ from those obtained for the linear or fully branched systems. With 20% SiR monomers present, mainly short linear and monocyclic compounds are formed, see Fig. 10. However, the average cluster size is larger than in the linear case, and already some clusters of genus two and three, i.e. bicyclic and tricyclic systems are found. When the number of branching points is increased to 80%, the average cluster size and the genus increase considerably. This demonstrates once again that incorporation of trifunctional (SiR) monomers leads to a structure with interconnected and fused rings. Hence, the results for the hybrid polysilane and polysilyne networks show that this class of materials is built up from cyclic structures interconnected via short linear chains.

An interesting question is to what extent the structure of the polysilyne depicted in Fig. 8 is consistent with the flexibility of polysilynes such as indicated by its thermal properties, i.e. whether the structure allows for conformational changes affecting the degree of σ -conjugation. Although at first sight the network of fused cyclic structures seems to be quite rigid, there are a number of features which suggest a certain degree of flexibility. Firstly, some (short) linear fragments and extended cyclic structures, both of which imply conformational flexibility, are distinguishable in Fig. 8. Secondly, there is also a number of rings which are interconnected by a single Si-Si bond. This should give the possibility for rings to rotate with respect to each other; i.e., the structure depicted in Fig. 8 is not rigid. A third factor which may contribute to the flexibility of the networks is that silicon rings are known to be highly flexible. In this context it is of interest that even in the solid state dodecamethylcyclohexasilane

$\text{Si}_6\text{Me}_{12}$ undergoes a rapid ring inversion [24]. While it is not likely that ring inversions occur for fused ring systems, they might be possible for rings connected to linear chains or connected to other rings by a single Si-Si bond.

Hence, the networks obtained in our simulations are already flexible. However, there are a number of reasons why experimentally prepared polysilynes can even more easily undergo conformational changes. A preferred polymer extension at the termini of the already formed polymer, as discussed above, will enhance chain growth rather than branching. This will have the consequence that polysilynes in reality may contain more linear chains and larger cyclic structures than depicted in Fig. 8. Another factor is the size of the organic side group R. While in the simulations R has the dimensions of a methyl group, much more bulky side groups such as hexyl, isobutyl and phenyl substituents have been used in experimental studies [9,7]. If bulky side groups are present the network is expected to be less dense and to incorporate more linear fragments than in the present case.

A question left to be answered is whether polysilynes obtained by a Wurtz-type condensation should be regarded as one, two or three-dimensional silicon materials. At first sight, the silicon network in Fig. 8 percolates in three dimensions. However, the description of the simulated polysilyne and hybrid polysilane/polysilyne networks by $g = 1 + e - n$, which is Euler's equation for two-dimensional networks [25], implies that topologically the silicon backbones of these materials are best regarded as two-dimensional systems. This is consistent with the electronic spectra which approach that of an indirect band gap semiconductor [6-8].

In summary, we have shown that the formation and structure of polysilanes, polysilynes and hybrid-polysilane/polysilyne networks can be adequately described by a simulation based on rare event dynamics of diffusion and reaction steps. The simulations indicate that ring formation is an important factor for all three types of silicon materials. Insight has been obtained in the conformational flexibility of polysilynes and polysilane/polysilyne materials such as inferred from experimental studies. It is anticipated that simulations can provide an even more comprehensive picture when variation of the size of the organic substituent R and differences in reactivity of different types of Si-Cl functionalities are implemented. This would be the subject of further work.

[1] L. Brus, *J. Phys. Chem.* **98**, 3575 (1994).
 [2] R. West, in *Comprehensive Organometallic Chemistry II*, E. Abe, F.G.A. Stone and G. Wilkinson (Eds.), Vol. 2, Pergamon, Oxford, p. 77 (1995).

- [3] R.D. Miller and J. Michl, *Chem. Rev.* **89**, 1359 (1989).
- [4] R.G. Jones, R.E. Benfield, R.H. Cragg, A.C. Swain and S.J. Webb, *Macromolecules* **26** (1993), 4878.
- [5] P.A. Bianconi and T.W. Weidman, *J. Am. Chem. Soc.* **110**, 2342 (1988).
- [6] P.A. Bianconi, F.C. Schilling and T.W. Weidman, *Macromolecules* **22**, 1697 (1989).
- [7] K. Furukawa, M. Fujino and N. Matsumoto, *Macromolecules* **22**, 3423 (1990).
- [8] W.L. Wilson and T.W. Weidman, *Synth. Met.* **49-50**, 407 (1992).
- [9] C.A. van Walree, T.J. Cleij, L.W. Jenneskens, E.J. Vlietstra, G.P. van der Laan, M.P. de Haas and E.T.G. Lutz, *Macromolecules* **29**, 7362 (1996).
- [10] M. Sasaki and K. Matyjaszewski, *J. Polym. Sci., Part A: Polym. Chem.* **33**, 771 (1995).
- [11] W.L. Wilson and T.W. Weidman, *J. Phys. Chem.* **95**, 4568 (1991).
- [12] A. Watanabe, H. Miike, Y. Tsusumi and M. Matsuda, *Macromolecules* **26**, 2111 (1993).
- [13] J. Maxka, J. Chrusciel, M. Sasaki and K. Matyjaszewski, *Macromol. Symp.* **77**, 79 (1994).
- [14] T.J. Cleij, S.K.Y. Tsang and L.W. Jenneskens, *Macromolecules* **32**, 3286 (1999).
- [15] J.B. Lambert, J.L. Pflug and C.L. Stern, *Angew. Chem. Int. Ed. Engl.* **34**, 98 (1995).
- [16] H. Suzuki, Y. Kimata, S. Satoh and A. Kuriyama, *Chem. Lett.* 293 (1995).
- [17] P.N. Keating, *Phys. Rev.* **145** (1966).
- [18] G.T. Barkema, M.J. Howard, and J.L. Cardy, *Phys. Rev. E* **53**, 2017 (1996).
- [19] N. Metropolis *et al.*, *J. Chem. Phys.* **21**, 1087 (1953).
- [20] J.M. Zeigler, *Polym. Prepr.* **27** (1986), 109.
- [21] L.F. Brough, R. West, *J. Am. Chem. Soc.* **103** (1981), 3049.
- [22] S.M. Chen, A. Katti, A. Blinka and R. West, *Synthesis* (1985), 684.
- [23] W. Uhlig, *Z. Naturforsch.* **50b**, 1674 (1995).
- [24] N. Casarini, L. Lunazzi and A. Mazzanti, *J. Org. Chem.* **63** (1998), 9125.
- [25] K. Devlin, in *The new golden age*, Penguin, UK, 1990.